VIA MEDICA

ORIGINAL ARTICLE

Folia Morphol.
Vol. 84, No. 4, pp. 902–914
DOI: 10.5603/fm.104773

ISSN 0015–5659
eISSN 1644–3284
journals.viamedica.pl

Facial nerve trunk surgical identification: a new approach

Angela Babuci[1], Silvia Stratulat[2], Zinovia Zorina[1], Ilia Catereniuc[1], Anastasia Bendelic[1], Nataliya Trushel[3], Oleg Solomon[4], Elena Stepco[5], Sergiu Calancea[6], Sofia Lehtman[7], Gabriela Motelica[7], Stanislav Strisca[7], Andrei Mostovei[7]

[1]*Department of Anatomy and Clinical Anatomy, Nicolae Testemitanu State University of Medicine and Pharmacy, Moldova*
[2]*Department of Biochemistry and Clinical Biochemistry, Nicolae Testemitanu State University of Medicine and Pharmacy, Chisinau, Moldova*
[3]*Department of Normal Anatomy, Belarussian State Medical University, Minsk, Belarus*
[4]*Ilarion Postolachi Department of Orthopaedic Stomatology, Nicolae Testemitanu State University of Medicine and Pharmacy, Chisinau, Moldova*
[5]*Ion Lupan Department of Paediatric Oral-Maxillofacial Surgery and Paedodontics, Nicolae Testemitanu State University of Medicine and Pharmacy, Chisinau, Moldova*
[6]*Light Dental Clinic, Bucharest, Romania*
[7]*Arsenie Gutan Department of Oral-Maxillofacial Surgery and Oral Implantology, Nicolae Testemitanu State University of Medicine and Pharmacy, Chisinau, Moldova*

[Received: 2 February 2025; Accepted: 31 March 2025; Early publication date: 22 April 2025]

Background: *Considering the lack of feasible methods for previsualisation of the extracranial portion of facial nerve and the high risk of its iatrogenic injuries, a better understanding of facial nerve identification landmarks is much needed. The aim of this study was to identify reliable landmarks for surgical access to the facial nerve trunk (FNT).*

Materials and methods: *Our study was conducted on 75 hemifaces of adult embalmed cadavers. Prior to anatomical dissection, the cephalometric type of each head was determined and the landmarks identified for study were established.*

Results: *For the FNT surgical access, eight landmarks were measured and statistically analysed against five criteria: gender, laterality, cephalometric type, branching pattern and its variant (classic/atypical). Six of the examined landmarks showed statistical significance depending on gender ($p \leq 0.05$), i.e.: angle of the FNT bifurcation (FNTB); distance between the FNT division and the angle of the mandible (FNTD/AM); distance between the FNT division and the apex of the mastoid process (FNTD/AMP); distance between the FNT origin and the intertragic notch (FNTO/ITN); distance between the FNT origin and the triangular prominence of the cartilage of the external acoustic meatus (FNTO/ΔCEAM); and distance between the FNT origin and the anterior margin of the sternocleidomastoid muscle insertion point (FNTO/AMSCMIP). The angle formed at the intersection of the facial nerve trunk with a vertical line drawn through the anterior margin of the external acoustic meatus (FNT/VEAM), was statistically significant depending on laterality ($p = 0.049$). The FNT bifurcation angle was also statistically significant depending on the branching pattern ($p = 0.005$).*

Address for correspondence: Angela Babuci, Nicolae Testemitanu State University of Medicine and Pharmacy, 165 Stefan cel Mare si Sfant Boulevard, MD-2004, Chisinau, Moldova; e-mail: angela.babuci@usmf.md

Conclusions: Six of the evaluated landmarks (75%) FNTB, FNTD/AM, FNTD/AMP, FNTO/ITN, FNTO/ΔCEAM and FNTO/AMSCMIP were statistically significant depending on gender and FNT/VEAM was significant depending on laterality. Based on the cephalometric type, the highest mean values were observed in the dolichocephalic type and the lowest in the brachycephalic type. (Folia Morphol 2025; 84, 4: 902–914)

Keywords: facial nerve, landmarks, gender, branching pattern, cephalometric type

INTRODUCTION

The motor fibres of the facial nerve are characterised by an increased susceptibility to various harmful factors, including a wide range of viruses, bacteria, somatic diseases, craniofacial trauma, tumours, abnormalities, variations of the stylomastoid foramen, and even dental anaesthesia [1, 6, 14, 34, 35]. The increasing expansion of the beauty industry has led to greater demand for aesthetic and cosmetic procedures with surgical interventions. These can have fatal consequences, due to the high degree of facial nerve variability [2, 25, 26, 36]. The frequency of facial nerve impairments in parotid tumours is explained by the topographical relationships of its extracranial branches with the glandular parenchyma.

In the classic variant, the FNT bifurcates into the temporofacial and cervicofacial divisions [25]. However, many researchers have reported tri-, quadri-, and plurifurcation patterns and also number variation of the facial nerve trunk [2, 13, 20, 23, 26, 36]. The lowest reported rate of facial trunk bifurcation was 75% [13], and the highest was 100% [25]. FNT trifurcation has been observed in 6.7–20% [20, 26, 38]. Iatrogenic injuries of the extracranial branches of the facial nerve vary from 0.4% (in arterial embolisation) up to 49.5% (in parotid surgery) [43] and from 1% to 20% in cosmetic surgery [32].

The most vulnerable to injuries are the temporofacial and cervicofacial divisions with their terminal ramifications. In contrast, due to its deep localisation, the facial nerve trunk is better protected [5]. Nevertheless, every surgeon should be aware of FNT variations [2, 13, 20, 23, 26, 36].

Now, the 'gold standard' in nerve repair is the use of sensory nerve grafts. For autologous nerve grafting, the most commonly used are the sural [22, 24], saphenous, and medial antebrachial cutaneous nerves [22], as well as the great auricular nerve (GAN) [7, 21, 24], which width correlates with the width of the facial nerve trunk [7, 21], demonstrating good results in repair of defects that do not exceed 7 cm in length. The anastomosis of the hypoglossal nerve to a branch of the facial nerve [27], and the hypoglossal-facial anastomosis at the bulbopontine angle, when the proximal stump of the facial nerve cannot be identified [24], is applied for the facial nerve repair.

Over the last decade, both the techniques and the quality of facial nerve repair have significantly improved. Thus, along with direct suturing, autografts and acellular allografts, tissue engineering [18, 37], and gene therapy [10] are now being used.

Excellent functional recovery for nerve grafting of gaps shorter than 2 cm has been obtained [22]. Good results were reported for autografts shorter than 4 cm, while for those of 4–6 cm, a success rate of 64% has been reported [29]. According to Kuffler et al. [22], there is a very poor regeneration across grafts of 8 cm in length, and no regeneration at all, across those longer than 10 cm. Moreover, Peters et al. [29] reported a success rate of 29% for autografts between 6–12 cm and 11% for those longer than 12 cm.

After nerve transection, as a result of fibrinogen diffusion from the leaky blood vessels and its combination with the thrombin, fibrinogen polymerisation and matrix formation occur, contributing to axon regeneration towards the distal nerve stump. It should be noted that a good functional recovery has been revealed when the repaired nerve was tension-free and the grafting was carried out no later than 14 days after lesion [22]. A correlation between the amplitude of the motor unit potential and the facial nerve function ($r = –6.078$, $p = 0.02$) was established by Li et al. [24].

In acute peripheral nerve injury, adipokine leptin has been identified as an upstream regulator in Schwann cells. This leads to a chain of metabolic reactions, with mitochondrial oxidative phosphorylation modulating the glial metabolism under the process of nerve regeneration [37]. Acellular nerve allografts are used in peripheral nerve repair, serving as a scaffold for cell migration, macrophages infiltration and angiogenesis activation. Accumulation of T cells and promotion of progenerative signalling leads to Schwann cells migration and interaction with fibroblasts. As a result, Schwann cells are arranged into cell cords, contributing

to myelination of axons, at the junction with the native nerve, while at the other end of the nerve, very few, or no axons have been noted [29].

Gene therapy is a promising tool that can be used for regeneration over long stretches of the peripheral nerves. The efficacy of gene therapy depends especially on the level of glial cell line-derived neurothrophic factor responsible for regulating neuronal differentiation, motoneuron survival, and axonal regeneration [10].

Experimentally, it has been demonstrated on rats that scaffold-free aligned dental pulp stem cells, due to expression of neurotrophic and growth factors, *via* engineering nerve conduits, supply trophic cues, thereby inducing axon regeneration across a critically-sized nerve defect [9].

In facial nerve surgery, one of the most important goals is preservation of its integrity. The intracranial portion of the facial nerve can be previsualised *via* non-invasive imaging methods such as computed tomography, magnetic resonance imaging and tractography [16, 17, 31, 42, 44], but previsualisation of the parotid plexus branches by regular imaging methods is impossible [42]. At the experimental level, three-dimensional constructive interference in steady state magnetic resonance imaging [15] and high-resolution ultrasonography [40] have shown positive results for previsualising the facial nerve trunk and its primary divisions. Transcutaneous and intraoperative ultra-high frequency ultrasound [30], using long-chain hyaluronic acid mixed with methylene blue as facial nerve markers has also been positive for the previsualisation of the zygomatic, buccal and marginal mandibular branches.

Considering the physical and psychological impacts on patients with irreversible injury of the facial nerve [3] and the impossibility of predicting the course of its extracranial branches, it is vital to increase our understanding of facial nerve anatomical variability and its identification landmarks.

MATERIALS AND METHODS

In order to identify feasible landmarks for facial nerve surgical access, 75 embalmed hemiheads of adult cadavers (59 male and 16 female) had been used. The anatomical dissection was carried out at the Department of Anatomy and Clinical Anatomy of Nicolae Testemitanu State University of Medicine and Pharmacy, Chisinau, Moldova. Prior to dissection, a selection of the intact heads, without any deformities, was made. The anteroposterior and biparietal dimensions of each head were carefully measured. For calculation of the cephalic index, the following formula was applied:

$$\textit{Cephalic index} = \frac{\textit{Transverse diameter} \times 100}{\textit{Longitudinal diameter}} \quad (1)$$

The cephalometric distribution of samples was carried out according to Franco et al. [12]. Samples with a cephalic index of up to 74.9 were classified as the dolichocephalic type (DCT), samples with a cephalic index of 75.0–79.9 were attributed to the mesocephalic type (MCT), and samples with a cephalic index over 80.0 were assigned to the brachycephalic type (BCT).

In order to identify feasible anatomical landmarks, the morphometry of the following parameters was taken: (1) angle of the FNT bifurcation (FNTB); (2) angle formed at the intersection of the facial nerve trunk with a vertical line drawn through the anterior margin of the external acoustic meatus (FNT/VEAM); (3) distance between the FNT division and the angle of the mandible (FNTD/AM); (4) distance between the FNT division and the apex of the mastoid process (FNTD/AMP); (5) distance between the FNT origin and the intertragic notch (FNTO/ITN); (6) distance between the FNT origin and the triangular prominence of the cartilage of the external acoustic meatus (FNTO/ΔCEAM); (7) distance between the FNT origin and the anterior margin of the sternocleidomastoid muscle insertion point (FNTO/AMSCMIP); and (8) distance between the FNT division and the posterior margin of the ramus of the mandible (FNTD/PMM) (Fig. 1).

A careful dissection of the soft tissues of the retromandibular fossa was performed. The depth of the dissection within the retromandibular fossa, until the moment when the facial nerve trunk was distinguishable in the dissection field, varied between 19–31 mm (FNTO/AMSCMIP).

After identification of the facial nerve trunk, dissection was carried out along its course to the level of its bifurcation into the temporofacial and cervicofacial divisions, continuing dissection along their ramifications. The angle of the FNT bifurcation, compared to the facial nerve trunk origin, is located more superficially and often appears first in the dissection field. Thus, in cases of difficulty in identifying the facial nerve trunk, its bifurcation angle was used as a landmark for dissection towards its origin. It should be noted that the capsule of the parotid gland and the superficial plane of the glandular parenchyma were crossed by numerous fine ramifications of the facial

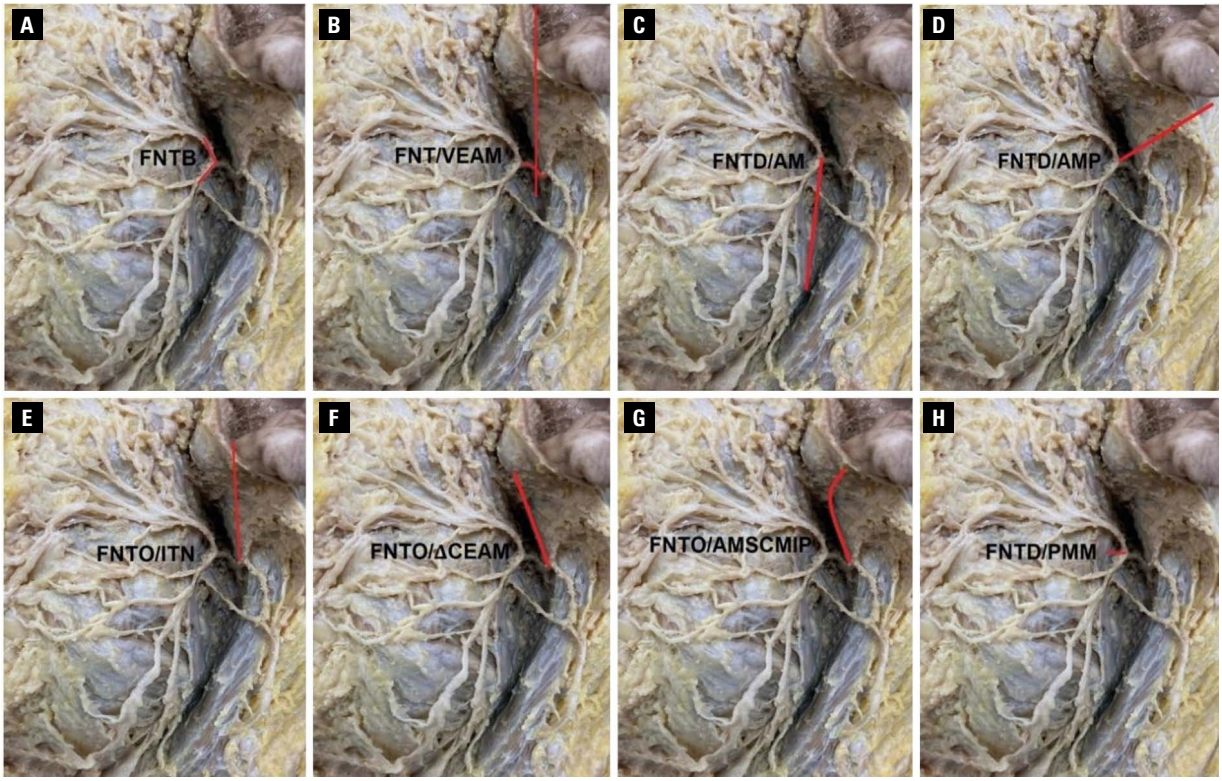

Figure 1. Landmarks for facial nerve trunk (FNT) surgical identification. FNTB — angle of FNT bifurcation; FNT/VEAM — angle formed at intersection of FNT with vertical line drawn through anterior margin of external acoustic meatus; FNTD/AM — distance between FNT division and angle of mandible; FNTD/AMP — distance between FNT division and apex of mastoid process; FNTO/ITN — distance between FNT origin and intertragic notch; FNTO/ΔCEAM — distance between FNT origin and triangular prominence of cartilage of external acoustic meatus; FNTO/AMSCMIP — distance between FNT origin and anterior margin of sternocleidomastoid muscle insertion point; FNTD/PMM — distance between FNT division and posterior margin of ramus of mandible.

nerve, and that the preservation of all the terminal twigs was impossible.

Every landmark was studied depending on five qualitative variables: gender, laterality, cephalometric type, branching pattern of the facial nerve and its variant (classic/atypical). Of the total sample size, 78.7% of specimens were male and 21.3% were female. Right hemifaces were 46.7% and left 53.3%. The mesocephalic type were 77.3%, dolichocephalic type 12%, and brachycephalic type 10.7%. The landmarks were evaluated depending on seven facial nerve branching patterns, with the following percentages: type I — 18.7%, type II — 14.7%, type III — 20.0%, type IV — 14.6%, type V — 5.3%, and type VI — 18.7%. Bizarre (non-identified) types, named by us 'atypical type NI', was determined in 8% of cases. It should be noted that each classic branching pattern, according to Davis classification [8], had an atypical pattern with a ratio of classic/atypical variant of 54.7:45.3%.

For statistical analysis of the quantitative and qualitative variables, predefined functions of Microsoft Excel, such as: AVERAGE, MEDIAN, STDEV, CONFIDENCE, QUARTILE, SKEW, CORELL, Student's *t*-test, χ^2 test and also one-way ANOVA, were used. The morphometry was taken twice by the same observer.

Table 1. Mean values of parameters of head depending on gender.

	Longitudinal diameter	Transverse diameter	Cephalic index
Males	195.5 mm	150.3 mm	76.9
Females	188.0 mm	147.2 mm	78.3
Difference	7.5	3.1	–1.4
p value	< 0.001	0.001	0.004

RESULTS

The head parameters were analysed using a one-way ANOVA test, and a statistically significant difference in head length between the cephalometric types ($p = 0.01$) was observed. The width of the head showed high significance ($p < 0.001$), and a very high degree of statistical significance was obtained for the cephalic index ($p < 0.0001$). The morphometric parameters showed a statistically significant difference depending on gender (Tab. 1).

Figure 2. Course of facial nerve trunk; **A.** Descending course; **B.** Horizontal course; **C.** Ascending course.

Table 2. Mean values of FNT identification landmarks depending on gender.

	FNTB (°)	FNT/VEAM (°)	FNTD/AM [mm]	FNTD/AMP [mm]	FNTO/ITN [mm]	FNTO/ΔCEAM [mm]	FNTO/AMSCMIP [mm]	FNTD/PMM [mm]
Males	120.3	118.5	44.3	19.3	33.1	13.8	24.5	9.6
Females	142.7	126.2	39.1	17.4	30.3	12.1	20.8	8.3
Difference	–224	–7.7	5.2	1.8	2.9	1.7	3.7	1.3
p value	0.050	0.440	< 0.001	< 0.001	< 0.001	0.007	< 0.001	0.269

FNT — facial nerve trunk; FNTB — angle of FNT bifurcation; FNT/VEAM — angle formed at intersection of FNT with vertical line drawn through anterior margin of external acoustic meatus; FNTD/AM — distance between FNT division and angle of mandible; FNTD/AMP — distance between FNT division and apex of mastoid process; FNTO/ITN — distance between FNT origin and intertragic notch; FNTO/ΔCEAM — distance between FNT origin and triangular prominence of cartilage of external acoustic meatus; FNTO/AMSCMIP — distance between FNT origin and anterior margin of sternocleidomastoid muscle insertion point; FNTD/PMM — distance between FNT division and posterior margin of ramus of mandible.

The cephalic index was also statistically significant depending on the facial nerve branching pattern ($p = 0.04$). However, depending on the side of the head and on the variant of branching (classic/atypical), the head parameters were not statistically significant ($p > 0.05$).

Three variants of the facial nerve trunk course were established in the current study: the descending course, the horizontal course, and the ascending course (Fig. 2). Understanding the variations of FNT course is of high clinical importance in terms of FNT surgical access. According to our experience, in both horizontal and ascending FNT courses, confusion and uncertainty about FNT intactness can occur. To avoid the FNT lesion, surgeons should keep in mind a possible variation of its course and for manipulations in the operative field, we would recommend the use of blunt dissection, from the FNT bifurcation angle towards the FNT.

The bifurcation angle of FNT into the temporofacial and cervicofacial divisions showed a statistically significant difference depending on gender ($p = 0.050$). Another statistically significant landmark was the distance between the origin of FNT and the triangular prominence of the cartilage of the external acoustic meatus ($p = 0.007$). The latter landmark proved to be one of the easiest to identify and due to its palpability and location in the field of the surgeon's vision, might be considered a high-fidelity landmark.

Highly significant depending on gender were: (1) the distance between the FNT division and the angle of the mandible ($p < 0.001$); (2) the distance between the FNT division and the apex of the mastoid process ($p < 0.001$); (3) the distance between the FNT origin and the intertragic notch ($p < 0.001$); and (4) the distance between the FNT origin and the anterior margin of the sternocleidomastoid muscle insertion point ($p < 0.001$) (Tab. 2).

Table 3. Mean values of FNT identification landmarks depending on branching pattern.

Landmark Branching pattern	FNTB [°] IGFV = 3.548; df = 6; p = 0.005		FNT/VEAM [°] IGFV = 0.886; df = 6; p = 0.511		FNTD/AM [mm] IGFV = 0.517; df = 6; p = 0.793		FNTD/AMP [mm] VFIG = 2.164; df = 6; p = 0.06	
	Mean ± SD	CI (95%)	Mean ± SD	CI (95%)	Mean ± SD	CI (95%)	Mean ± SD	CI (95%)
Type I	103.7 ± 23.60	90.3–117.1	130.6 ± 39.30	110.1–151.2	44.7 ± 4.44	42.3–47.1	18.5 ± 1.76	17.5–19.4
Type II	156.8 ± 29.24	139.5–174.1	135.3 ± 21.92	121.7–148.9	41.9 ± 3.56	39.8–44.0	19.1 ± 1.30	18.3–19.9
Type III	125.4 ± 37.97	103.9–146.9	117.4 ± 35.55	97.3–137.5	43.0 ± 3.46	41.2–44.8	19.4 ± 1.02	18.9–20.0
Type IV	108.7 ± 25.78	92.7–124.7	116.7 ± 38.35	94.1–139.4	43.0 ± 5.31	39.9–46.1	19.4 ± 2.16	18.1–20.6
Type V	135.7 ± 22.50	110.2–161.1	103.3 ± 40.62	63.4–143.1	43.0 ± 4.55	38.5–47.5	19.0 ± 1.41	17.6–20.4
Type VI	118.5 ± 35.03	97.8–139.2	111.1 ± 35.42	92.5–129,6	42.8 ± 4.87	40.2–45.3	17.7 ± 2.09	16.6–18.8
Type NI	135.4 ± 36.16	103.7–167.1	112.0 ± 31.33	81.3–142.7	44.3 ± 3.83	41.3–47.4	20.2 ± 1.94	18.6–21.7

CI — confidence interval; df — degree of freedom; FNT — facial nerve trunk; FNT/VEAM — angle formed at intersection of FNT with vertical line drawn through anterior margin of external acoustic meatus; FNTB — angle of FNT bifurcation; FNTD/AM — distance between FNT division and angle of mandible; FNTD/AMP — distance between FNT division and apex of mastoid process; IGFV — intergroup frequency variance; SD — standard deviation.

Table 4. Mean values of FNT landmarks depending on cephalometric type.

Landmark Cephalometric type	FNTB [°] IGFV = 0.085; df = 2; p = 0.919		FNT/VEAM [°] IGFV = 1.345; df = 2; p = 0.268		FNTD/AM [mm] VFIG = 2.086; df = 2; p = 0.132		FNTD/AMP [mm] IGFV = 1.201; df = 2; p = 0.307	
	Mean ± SD	CI (95%)	Mean ± SD	CI (95%)	Mean ± SD	CI (95%)	Mean ± SD	CI (95%)
MCT	125.0 ± 34.17	115.3–134.6	116.9 ± 37.04	107.2–126.7	43.6 ± 4.41	42.4–44.7	18.8 ± 1.78	18.4–19.3
BCT	119.1 ± 41.37	88.5–149.8	137.5 ± 19.14	124.2–150.8	40.4 ± 2.33	38.8–42.0	18.4 ± 1.06	17.6–19.1
DCT	123.9 ± 35.83	100.5–147.3	126.3 ± 25.73	107.2–145.3	43.6 ± 3.64	41.2–45.9	19.7 ± 2.35	18.1–21.2

BCT — brachycephalic type; CI — confidence interval; DCT — dolichocephalic type; df — degree of freedom; FNT — facial nerve trunk; FNT/VEAM — angle formed at intersection of FNT with vertical line drawn through anterior margin of external acoustic meatus; FNTB — angle of FNT bifurcation; FNTD/AM — distance between FNT division and angle of mandible; FNTD/AMP — distance between FNT division and apex of mastoid process; IGFV — intergroup frequency variance; MCT — mesocephalic type; SD — standard deviation.

In males, the mean value of the FNT bifurcation angle (FNTB) was 120.3°, while in females — 142.7° (p = 0.050). On right hemifaces, the bifurcation angle had a mean of 127.4° and on left ones — 121.2° (p = 0.483). The angle of FNT bifurcation was statistically significant, depending on the branching pattern (p = 0.005). For the classic branching pattern, the FNTB was 119.7°, and for the atypical variants it was 130.4° (p = 0.225). The morphometric parameters of the FNTB landmark depending on the branching pattern are set out in Table 3, and those depending on the cephalometric type are set out in Table 4.

The angle formed at the intersection of the facial nerve trunk with a vertical line drawn through the anterior margin of the external acoustic meatus (FNT/VEAM) in males had a mean of 118.5° and in females it was 126.2° (p = 0.440). Although no statistically significant gender difference was established for the FNT/VEAM, it is important to note that it was statistically significant depending on the laterality criterion (p = 0.049). On right hemiheads, the mean value of the FNT/VEAM was 110.8° and on left ones it was 127.3°. The mean values of the FNT/VEAM depending on the branching pattern are set out in Table 3 and those depending on the cephalometric type are set out in Table 4. In cases of classic branching patterns, the angle between FNT and VEAM was 125.4° and for the atypical patterns it was 112.9° (p = 0.138).

The mean distance between the facial nerve trunk division into its primary branches and the angle of the mandible (FNTD/AM) in males was 44.3 mm and in females it was 39.1 mm (p < 0.001). On right hemifaces, the mean value of the given landmark was 43.1 mm and on the left ones it was 43.4 mm (p = 0.761). The mean values of the FNTD/AM depending on the branching pattern are set out in Table 3, while those depending on the cephalometric type are set out in Table 4. For classic branching patterns, the FNTD/AM was 42.7 mm and for the atypical variants it was 43.9 mm (p = 0.208).

Table 5. Mean values of facial nerve trunk (FNT) landmarks depending on branching pattern.

Landmark Branching pattern	FNTO/ITN [mm] IGFV = 1.188; df = 6; p = 0.324		FNTO/ΔCEAM [mm] IGFV = 0.452; df = 6; p = 0.841		FNTO/AMSCMIP [mm] IGFV = 0.816; df = 6; p = 0.562		FNTD/PMM [mm] IGFV = 1.086; df = 6; p = 0.380	
	Mean ± SD	CI (95%)	Mean ± SD	CI (95%)	Mean ± SD	CI (95%)	Mean ± SD	CI (95%)
Type I	32.8 ± 3.14	31.1–34.4	13.4 ± 2.41	12.1–14.6	24.1 ± 3.43	22.3–25.9	9.6 ± 4.31	7.3–12.0
Type II	31.5 ± 2.84	29.8–33.1	13.6 ± 2.11	12.4–14.9	23.3 ± 4.10	20.8–25.7	11.7 ± 4.34	9.2–14.3
Type III	33.6 ± 2.21	32.4–34.7	13.6 ± 1.82	12.7–14.6	24.9 ± 2.50	23.6–26.2	7.9 ± 3.23	6.2–9.5
Type IV	32.5 ± 1.92	31.4–33.7	13.2 ± 1.94	12.0–14.3	22.5 ± 1.37	21.7–23.4	8.4 ± 5.22	5.3–11.4
Type V	31.8 ± 2.99	28.8–34.7	13.8 ± 4.11	9.7–17.8	23.5 ± 4.43	19.2–27.8	10.5 ± 3.51	7.1–13.9
Type VI	31.8 ± 2.46	30.5–33.1	12.8 ± 2.58	11.4–14.1	23.3 ± 3.22	21.6–25.0	9.1 ± 4.33	6.9–11.4
Type NI	33.7 ± 2.25	31.9–35.5	14.5 ± 2.51	12.5–16.5	24.8 ± 3.60	22.0–27.7	9.2 ± 2.23	7.4–10.9

CI — confidence interval; df — degree of freedom; FNTD/PMM — distance between FNT division and posterior margin of ramus of mandible; FNTO/ΔCEAM – distance between FNT origin and triangular prominence of cartilage of external acoustic meatus; FNTO/AMSCMIP — distance between FNT origin and anterior margin of sternocleidomastoid muscle insertion point; FNTO/ITN — distance between FNT origin and intertragic notch; IGFV — intergroup frequency variance; SD — standard deviation.

Table 6. Mean values of facial nerve trunk (FNT) landmarks depending on cephalometric type.

Landmark Cephalometric type	FNTO/ITN [mm] IGFV = 0.590; df = 2; p = 0.557		FNTO/ΔCEAM [mm] IGFV = 1.065; df = 2; p = 0.350		FNTO/AMSCMIP [mm] IGFV = 0.671; df = 2; p = 0.514		FNTD/PMM [mm] IGFV = 0.777; df = 2; p = 0.464	
	Mean ± SD	CI (95%)	Mean ± SD	CI (95%)	Mean ± SD	CI (95%)	Mean ± SD	CI (95%)
MCT	32.5 ± 2.61	31.8–33.2	13.6 ± 2.38	13.0–14.2	23.8 ± 2.96	23.0–24.6	9.3 ± 4.23	8.2–10.4
BCT	31.8 ± 2.71	29.9–33.6	12.6 ± 1.92	11.3–14.0	22.6 ± 4.10	19.8–25.5	7.8 ± 3.28	5.5–10.0
DCT	33.1 ± 2.26	31.6–34.6	12.8 ± 1.79	11.6–13.9	24.3 ± 3.57	22.0–26.7	10.2 ± 4.32	7.4–13.0

MCT — mesocephalic type; BCT — brachycephalic type; DCT — dolichocephalic type; df — degree of freedom; FNTD/PMM — distance between FNT division and posterior margin of ramus of mandible; FNTO/ΔCEAM — distance between FNT origin and triangular prominence of cartilage of external acoustic meatus; FNTO/AMSCMIP — distance between FNT origin and anterior margin of sternocleidomastoid muscle insertion point; FNTO/ITN — distance between FNT origin and intertragic notch; IGFV — intergroup frequency variance; MCT — mesocephalic type; SD — standard deviation.

The distance between the facial nerve trunk division and the apex of the mastoid process (FNTD/AMP), in males was 19.3 mm and in females it was 17.4 mm ($p < 0.001$). On right hemifaces, the mean value was 19.0 mm and on left ones — 18.1 mm ($p = 0.677$). The mean parameters of the FNTD/AMP depending on the branching pattern are set out in Table 3 and those depending on the cephalometric type are set out in Table 4. In classic branching patterns, the FNTD/AMP was 18.6 mm and in atypical variants it was 19.2 mm ($p = 0.155$).

The mean distance between the facial nerve trunk origin and the intertragic notch (FNTO/ITN), in males was 33.1 mm and in females was 30.3 mm, with a highly statistically significant difference ($p < 0.001$). On right hemifaces, the FNTO/ITN had a mean of 32.4 mm and on the left ones it was 32.6 mm ($p = 0.673$). The mean parameters of the FNTO/ITN based on the branching pattern are set out in Table 5, and those depending on the cephalometric type are set out in Table 6. In classic branching patterns, FNTO/ITN was 32.3 mm and in atypical variants it was 32.7 mm ($p = 0.487$).

The mean distance between the facial nerve trunk origin and the triangular prominence of the cartilage of the external acoustic meatus (FNTO/ΔCEAM), in males it was 13.8 mm and in females it was 12.1 mm, with a statistically significant difference depending on gender ($p = 0.007$). On right hemifaces, the mean value of the FNTO/ΔCEAM was 13.4 mm, while on left ones it was 13.5 mm ($p = 0.883$). The mean values of the FNTO/ΔCEAM depending on the branching pattern are set out in Table 5, and those depending on the cephalometric type are set out in Table 6. In classic variants of branching patterns, the FNTO/ΔCEAM was 13.1 mm and in atypical variants — 13.8 mm ($p = 0.158$).

The mean distance between the facial nerve trunk origin and the anterior margin of the sternocleidomastoid muscle insertion point (FNTO/AMSCMIP) in males it had a mean value of 24.5 mm and in females — 20.8 mm. A statistically significant difference of FNTO/AMSCMIP based on gender was determined ($p < 0.001$). On right samples, the FNTO/AMSCMIP was 23.7 mm and on left ones it was 23.8 mm ($p = 0.934$). The mean values of the FNTO/AMSCMIP depending on the branching pattern are set out in Table 5, while those depending on the cephalometric type are set out in Table 6. In classic branching patterns, the FNTO/AMSCMIP was 24.1 mm and in atypical variants was 23.3 mm ($p = 0.259$).

The mean distance between the facial nerve trunk division and the posterior margin of the ramus of the mandible (FNTD/PMM) in males was 9.6 mm and in females was 8.3 mm ($p = 0.269$). Bilaterally, the FNTD/PMM was 9.3 mm ($p = 0.980$). The mean values of the FNTD/PMM depending on the branching pattern are set out in Table 5 and those based on the cephalometric type are set out in Table 6. In classic variants of the facial nerve branching patterns, the FNTD/PMM was 9.2 mm, and in atypical variants it was 9.3 mm ($p = 0.952$).

The central tendency and frequencies variation of the analysed landmarks, in cases of symmetrical distribution, were represented by the mean value and standard deviation, while in cases of asymmetrical distribution, they were represented by the median and interquartile range (IQR) (Fig. 3).

Given that harvesting the sural nerve during facial nerve surgery involves an extended surgical field, in our opinion the urgent FNT repair with the great auricular nerve, would be more suitable, because its width bilaterally correlates with the width of the FNT [7, 21]. Alongside the laterality criterion, we also examined correlation of their width depending on gender and cephalometric type.

The mean width of the FNT was 2.7 ± 0.47 mm and the mean width of the GAN was 2.9 ± 0.51 mm. Statistical analysis of the morphometric parameters demonstrated a very strong positive correlation ($r = +0.86$) between the width of the FNT and the width of the GAN, with a high statistical significance ($p < 0.001$). A positive and very strong correlation between the width of the FNT and the width of the GAN was determined in both males and females. In males, the Pearson's correlation coefficient was positive ($r = +0.78$) ($p < 0.001$), while in females it was also positive, but stronger comparing to males ($r = +0.98$) ($p < 0.001$) (Fig. 4). A strong correlation between the width of the FNT and that of the GAN, based on laterality, was observed. On right hemifaces, the Pearson's correlation coefficient was ($r = +0.93$) and on the left side it was ($r = +0.81$), statistically significant on

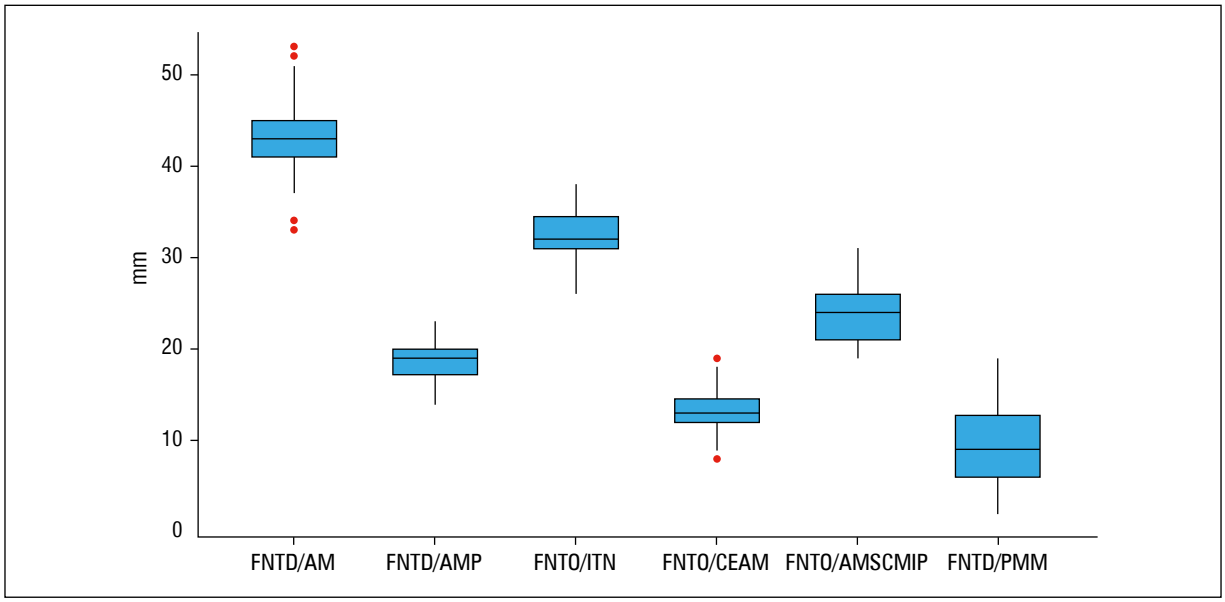

Figure 3. Central tendency and variation of facial nerve trunk (FNT) identification landmarks. FNTD/AM — distance between FNT division and angle of mandible; FNTD/AMP — distance between FNT division and apex of mastoid process; FNTO/ITN — distance between FNT origin and intertragic notch; FNTO/ΔCEAM — distance between FNT origin and triangular prominence of cartilage of external acoustic meatus; FNTO/AMSCMIP — distance between FNT origin and anterior margin of sternocleidomastoid muscle insertion point; FNTD/PMM — distance between FNT division and posterior margin of ramus of mandible.

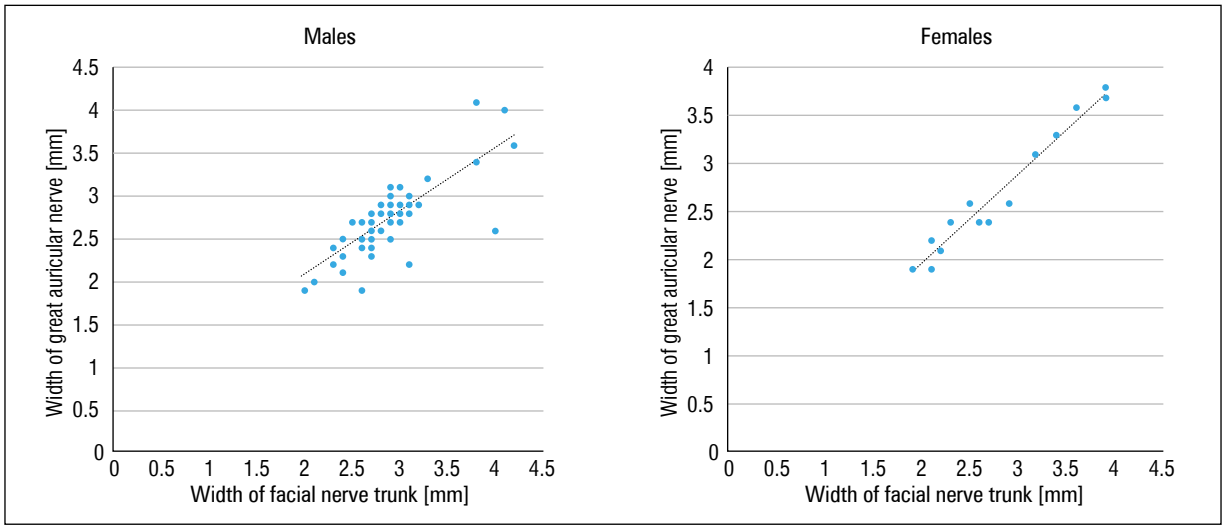

Figure 4. Correlation between width of facial nerve trunk and width of great auricular nerve depending on gender.

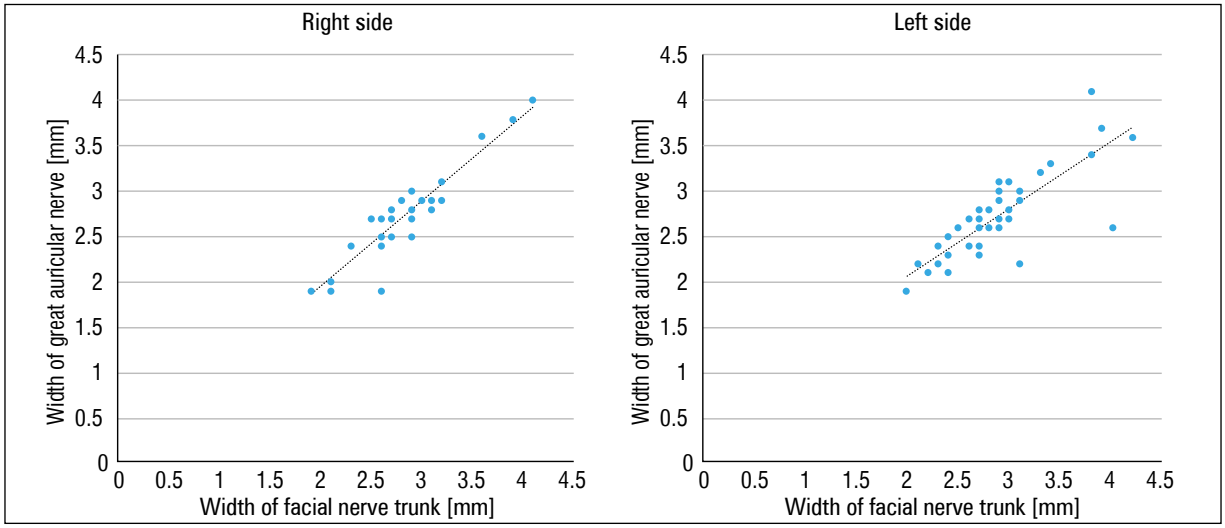

Figure 5. Correlation between width of facial nerve trunk and width of great auricular nerve depending on laterality.

each side of the head ($p < 0.001$). The correlation was stronger on right samples ($p = 0.05$) (Fig. 5). Depending on the cephalometric type, the lowest correlation coefficient between the width of the FNT and the width of the GAN was established in MCT ($r = +0.84$). A higher correlation coefficient was determined in BCT ($r = +0.91$), and in DCT the correlation coefficient was the highest of all ($r = +0.94$) (Fig. 6). All the cephalometric types showed a strong statistically significant correlation between the width of the FNT and the width of the GAN, for MCT ($p < 0.001$), and for each of the BCT and DCT ($p = 0.002$). No significant difference was determined between the correlation coefficients of the cephalometric types ($p > 0.05$).

DISCUSSION

Various anatomical structures are used as landmarks for the surgical identification of the facial nerve trunk [4, 11, 12, 19, 28, 39, 41], classified by us into three groups: soft landmarks (blood vessels, nerves, ligaments and muscles); hard landmarks (cartilaginous and bony structures); and 'projection' landmarks (diverse geometric figures: triangles, quadrilaterals and etc.). Unfortunately, in the majority of papers, the well-known landmarks are given and only in a few papers have been published new landmarks [4, 15]. Among the most common landmarks reported have been the posterior belly of the digastric muscle, the stylomastoid artery, the retromandibular and superficial

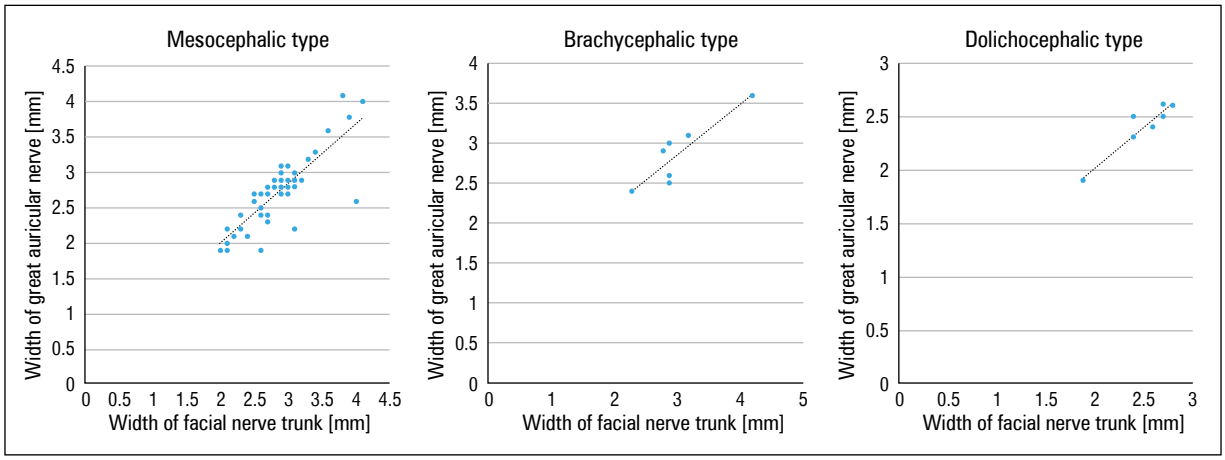

Figure 6. Correlation between width of facial nerve trunk and width of great auricular nerve depending on cephalometric type.

temporal veins, the mastoid and styloid processes, the angle and the ramus of the mandible [11, 12, 39, 41].

Data concerning the FNT bifurcation angle, which in our opinion could serve as a landmark for FNT surgical identification, has scarcely been reported in the literature. According to Khoa et al. [20], the mean value of the FNT bifurcation angle was 91.2°. In 66.7% of cases, the angle was sharp, and in 33.3% of cases it was obtuse. In our study, the FNT bifurcation angle had a mean of 120.3° in males and 142.7° in females, a difference which was statistically significant ($p = 0.050$).

The distance between the FNT and the tragus varies between 10–20 mm, and even if its fidelity index is 20% only [41], the importance of the tragus as a landmark should not be overlooked [4]. According to Zhong et al. [45], the distance between the FNT and the external acoustic meatus was 14.2 ± 1.8 mm.

In our study, a new landmark was identified, which is the distance between the origin of the facial nerve trunk and the intertragic notch. It should be noted that this landmark demonstrated a high statistical significance ($p < 0.001$) depending on gender. In males, the mean value of the named landmark was 33.1 mm, while in females it was 30.3 mm.

One of the most used landmarks for FNT identification is the mastoid process. A mean value of 12.5 ± 2.3 mm for the distance between the FNT origin and the apex of the mastoid process was reported by Stankevicius [36]. Zhong et al. [45] obtained a mean of 14.1 ± 1.8 mm, Kwak et al. [23] reported 21.0 ± 3.1 mm, Witt et al. [41] revealed 23.0 mm, and the highest values were reported by Khoa et al. [20], who obtained a mean of 28.9 mm on the right and 25.1 mm on the left. In the current study, as a landmark, the distance between the FNT division into its primary branches and the apex of the mastoid process was measured, obtaining a mean of 18.9 ± 1.8 mm ($p < 0.001$).

The variability of the facial nerve is not limited to the nerve itself, it is also extrapolated to its identification landmarks. We consider that among the factors of major clinical significance is the width of the soft tissues covering the facial nerve trunk. Thus, as a new FNT identification landmark, the distance between the FNT origin and the anterior margin of the sternocleidomastoid muscle insertion point was proposed. In males, FNTO/AMSCMIP was 24.5 mm, and in females it was 20.8 mm. FNTO/AMSCMIP showed a high statistical significance depending on gender ($p < 0.001$). As feasible landmarks, the tympanomastoid fissure and the triangular cartilaginous prominence of the external acoustic meatus have been recommended [41].

In the current study, the triangular prominence of the cartilage of the external acoustic meatus proved to be reliable both morphometrically and in terms of accessibility during dissection. The distance between the triangular prominence of the cartilage of the external acoustic meatus and the origin of the FNT in males was 13.8 mm, and in females was 12.1 mm. A statistically significant difference based on gender was determined for this landmark ($p = 0.007$).

According to Naidu et al. [26], the morphometric parameters of anatomical landmarks depend on gender and laterality, although some authors have recommended taking into consideration also ethnicity [33, 38]. A mean value of 36.45 ± 4.14 mm for the distance between the FNT bifurcation and the angle

of the mandible was reported by Stankevicius [36], while Khoa et al. [20], obtained a mean of 40.8 mm. For the distance between the FNT origin and the angle of the mandible in males, Naidu et al. [26] obtained a mean value of 47.5 ± 4.7 mm and in females it was 39.7 ± 8.3 mm ($p < 0.001$). On the right side in males, the mean value was 45.1 mm, and on the left side it was 42.9 mm ($p < 0.002$). In our study, the mean distance between the facial nerve trunk division and the angle of the mandible in males was 44.3 mm, and in females was 39.1 mm ($p < 0.001$). On the right side, the named landmark had a mean of 43.1 mm, and on the left, it was 44.4 mm ($p = 0.252$). We consider that the divergences and variations in these reported data could be related to facial nerve individual variability and ethnicity-specific features.

Taking into consideration that there is a strong bilateral correlation between the widths of the FNT and GAN [7, 21], the great auricular nerve can be used both as a predictor for FNT width and as a graft in FNT repair. Colbert et al. [7], for the GAN obtained a width of 2.75 ± 0.53 mm, and for the FNT it was 2.83 ± 0.54 mm. Correlation on left hemifaces was $r = 0.934$ ($p < 0.001$), and on the right – $r = 0.940$ ($p < 0.001$). Kriengkraikasem et al. [21], for the GAN reported a width of 3.26 ± 0.67 mm, and for the FNT – 3.36 ± 0.71 mm. A correlation of $r = 0.740$ ($p = 0.002$) was determined on the right side, while on the left hemifaces it was $r = 0.839$ ($p < 0.001$).

In the current study, a strong and statistically significant correlation between the width of the FNT, with a mean value of 2.7 ± 0.47 mm, and that of the GAN, with a mean of 2.9 ± 0.51 mm, across all the investigated criteria i.e. laterality, gender and cephalometric type ($p < 0.001$), was determined.

We must emphasise that in our sample group, the width of the great auricular nerve exceeded the width of the facial nerve trunk, which does not align with the data reported by Colbert et al. [7] and Kriengkraikasem et al. [21].

For optimisation of the facial nerve trunk identification and to minimize the risk of iatrogenic injury, we recommend taking into consideration FNT-specific features such as: its exit angle from the facial canal (sharp, right, obtuse) [1]; the course of the FNT (descending, horizontal, ascending) [2]; the variation of the FNT ramification into primary branches (bifurcation, trifurcation, multifurcation); and also its numerical variants.

CONCLUSIONS

The anatomical landmarks for facial nerve trunk identification investigated in this study have demonstrated practicality at the application level, by being palpable, easy to measure, and always in the surgeon's field of view. Six of the evaluated landmarks (75%) FNTB, FNTD/AM, FNTD/AMP, FNTO/ITN, FNTO/ΔCEAM and FNTO/AMSCMIP were statistically significant depending on gender and FNT/VEAM was significant depending on laterality. Based on the cephalometric type, the highest mean values were observed in the dolichocephalic type and the lowest in the brachycephalic type.

Alongside the obtained results, the limitations of our study include: a small number of hemifaces, almost three times as many male samples as female ones and predominance of mesocephalic type individuals.

ARTICLE INFORMATION AND DECLARATIONS

Data availability statement

The data generated in this study is available upon request.

Ethics statement

This research project was conducted according to the ethical principles of the Declaration of Helsinki for medical research and it was approved by the Ethics Committee of Nicolae Testemitanu State University of Medicine and Pharmacy, Chisinau, Moldova.

Author contributions

Conceptualisation: ABa. Methodology: ABa, AM. Resources: ABa, ABe, ZZ, IC. Software: ABa, SStri, AM. Validation: ABa, AM. Formal analysis: ABa, SStra, ABe, ZZ, IC. Investigation: ABa, AM. Writing — original draft: ABa, SStra, ABe, ZZ, IC, NT, OS, ES, SC, SL, GM, SStri, AM. Writing — editing: ABa, SStra, ABe, ZZ, IC, NT, OS, ES, SC, SL, GM, SStri, AM. Supervision: ABa, AM. Project administration: ABa, AM. Final version approval: all authors.

Funding

This research received no specific grant from any funding agency in the public, commercial, or non-profit sectors.

Acknowledgments

The authors would like to express our gratitude to the cadavers used in our research.

Conflict of interest

The authors declare no conflict of interest.

REFERENCES

1. Babuci A, Ashkar L, Zorina Z, et al. Anatomical features of the mastoid segment of the facial canal. Folia Morphol. 2025; 84(1): 117–126, doi: 10.5603/fm.100260, indexed in Pubmed: 38842075.
2. Babuci A, Catereniuc I, Zorina Z, et al. Morphology and variability of the facial nerve trunk depending on the branching pattern, gender, anthropometric type and side of the head in Moldovan population. Folia Morphol. 2023; 82(4): 791–797, doi: 10.5603/FM.a2022.0088, indexed in Pubmed: 36254108.
3. Baker DC, Conley J. Avoiding facial nerve injuries in rhytidectomy. Anatomical variations and pitfalls. Plast Reconstr Surg. 1979; 64(6): 781–795, doi: 10.1097/00006534-197912000-00005, indexed in Pubmed: 515227.
4. Borle RM, Jadhav A, Bhola N, et al. Borle's triangle: a reliable anatomical landmark for ease of identification of facial nerve trunk during parotidectomy. J Oral Biol Craniofac Res. 2019; 9(1): 33–36, doi: 10.1016/j.jobcr.2018.08.004, indexed in Pubmed: 30191119.
5. Castañares S. Facial nerve paralyses coincident with, or subsequent to, rhytidectomy. Plast Reconstr Surg. 1974; 54(6): 637–643, doi: 10.1097/00006534-197412000-00001, indexed in Pubmed: 4438462.
6. Chisci G, Chisci D, Chisci E, et al. Facial nerve palsy after inferior alveolar nerve block: a rare presentation of ocular complication and literature review. Reports. 2023; 6(4): 47, doi: 10.3390/reports6040047.
7. Colbert S, Parry DA, Hale B, et al. Does the great auricular nerve predict the size of the main trunk of the facial nerve? A clinical and cadaveric study. Br J Oral Maxillofac Surg. 2014; 52(3): 230–235, doi: 10.1016/j.bjoms.2013.12.001, indexed in Pubmed: 24373335.
8. Davis RA, Anson BJ, Budinger JM, et al. Surgical anatomy of the facial nerve and parotid gland based upon a study of 350 cervicofacial halves. Surg Gynecol Obstet. 1956; 102(4): 385–412, indexed in Pubmed: 13311719.
9. Drewry MD, Shi D, Dailey MT, et al. Enhancing facial nerve regeneration with scaffold-free conduits engineered using dental pulp stem cells and their endogenous, aligned extracellular matrix. J Neural Eng. 2024; 21(5), doi: 10.1088/1741-2552/ad749d, indexed in Pubmed: 39197480.
10. Eggers R, de Winter F, Tannemaat MR, et al. GDNF gene therapy to repair the injured peripheral nerve. Front Bioeng Biotechnol. 2020; 8: 583184, doi: 10.3389/fbioe.2020.583184, indexed in Pubmed: 33251197.
11. El Kininy W, Davy S, Stassen L, et al. Novel variations in spatial relations between the facial nerve and superficial temporal and maxillary veins. Folia Morphol. 2018; 77(4): 775–779, doi: 10.5603/FM.a2018.0019, indexed in Pubmed: 29500899.
12. Franco FC, de Araujo TM, Vogel CJ, et al. Brachycephalic, dolichocephalic and mesocephalic: Is it appropriate to describe the face using skull patterns? Dental Press J Orthod. 2013; 18(3): 159–163, doi: 10.1590/s2176-94512013000300025, indexed in Pubmed: 24094027.
13. Gaughran GR. The parotid compartment. Ann Otol Rhinol Laryngol. 1961; 70: 31–51, doi: 10.1177/000348946107000103, indexed in Pubmed: 13703964.
14. Ghosh SK, Narayan RK. Variations in the morphology of stylomastoid foramen: a possible solution to the conundrum of unexplained cases of Bell's palsy. Folia Morphol. 2021; 80(1): 97–105, doi: 10.5603/FM.a2020.0019, indexed in Pubmed: 32073133.
15. Guenette JP, Ben-Shlomo N, Jayender J, et al. MR imaging of the extracranial facial nerve with the CISS sequence. AJNR Am J Neuroradiol. 2019; 40(11): 1954–1959, doi: 10.3174/ajnr.A6261, indexed in Pubmed: 31624121.
16. Gupta S, Mends F, Hagiwara M, et al. Imaging the facial nerve: a contemporary review. Radiol Res Pract. 2013; 2013: 248039, doi: 10.1155/2013/248039, indexed in Pubmed: 23766904.
17. Hilly O, Chen JM, Birch J, et al. Diffusion tensor imaging tractography of the facial nerve in patients with cerebellopontine angle tumors. Otol Neurotol. 2016; 37(4): 388–393, doi: 10.1097/MAO.0000000000000984, indexed in Pubmed: 26905823.
18. Huang H, Lin Q, Rui Xi, et al. Research status of facial nerve repair. Regen Ther. 2023; 24: 507–514, doi: 10.1016/j.reth.2023.09.012, indexed in Pubmed: 37841661.
19. Joseph ST, Sharankumar S, Sandya CJ, et al. Easy and safe method for facial nerve identification in parotid surgery. J Neurol Surg B Skull Base. 2015; 76(6): 426–431, doi: 10.1055/s-0035-1549001, indexed in Pubmed: 26682121.
20. Khoa TD, Bac ND, Luong HV, et al. Anatomical characteristics of facial nerve trunk in Vietnamese adult cadavers. Open Access Maced J Med Sci. 2019; 7(24): 4230–4238, doi: 10.3889/oamjms.2019.366, indexed in Pubmed: 32215069.
21. Kriengkraikasem K, Kowitwibool K, Chanpoo M. Variation of the great auricular nerve and prediction of the facial nerve trunk size. Plast Reconstr Surg Glob Open. 2018; 6(12): e2000, doi: 10.1097/GOX.0000000000002000, indexed in Pubmed: 30656105.
22. Kuffler DP, Foy C. Restoration of neurological function following peripheral nerve trauma. Int J Mol Sci. 2020; 21(5), doi: 10.3390/ijms21051808, indexed in Pubmed: 32155716.
23. Kwak HH, Park HD, Youn KH, et al. Branching patterns of the facial nerve and its communication with the auriculotemporal nerve. Surg Radiol Anat. 2004; 26(6): 494–500, doi: 10.1007/s00276-004-0259-6, indexed in Pubmed: 15368081.
24. Li Li, Fan Z, Wang H, et al. Efficacy of surgical repair for the functional restoration of injured facial nerve. BMC Surg. 2021; 21(1): 32, doi: 10.1186/s12893-021-01049-x, indexed in Pubmed: 33419427.
25. Martínez Pascual P, Maranillo E, Vázquez T, et al. Extracranial course of the facial nerve revisited. Anat Rec (Hoboken). 2019; 302(4): 599–608, doi: 10.1002/ar.23825, indexed in Pubmed: 29659175.
26. Naidu L, Rennie CO. The extracranial course of the facial nerve and bony anatomical landmarks for localization of the facial nerve trunk during parotidectomies. Eur J Anat. 2020; 24(1): 37–48.

27. Neamonitou F, Kotrotsiou M, Stavrianos S. Correction: dynamic surgical restoration of mid and lower facial paralysis: a single-Greek-centre experience. Cureus. 2025; 17(2): c212, doi: 10.7759/cureus.c212, indexed in Pubmed: 39974297.
28. Pereira JA, Merí A, Potau JM, et al. A simple method for safe identification of the facial nerve using palpable landmarks. Arch Surg. 2004; 139(7): 745–747; discussion 748, doi: 10.1001/archsurg.139.7.745, indexed in Pubmed: 15249407.
29. Peters BR, Wood MD, Hunter DA, et al. Acellular nerve allografts in major peripheral nerve repairs: an analysis of cases presenting with limited recovery. Hand (N Y). 2023; 18(2): 236–243, doi: 10.1177/15589447211003175, indexed in Pubmed: 33880944.
30. Poelaert J, Coopman R, Ureel M, et al. Visualization of the facial nerve with ultra-high-frequency ultrasound. Plast Reconstr Surg Glob Open. 2023; 11(12): e5489, doi: 10.1097/GOX.0000000000005489, indexed in Pubmed: 38115834.
31. Radomska K, Mielnik M, Gawlikowska-Sroka A, et al. Selected structures of middle ear relevant to cochlear implantation on the basis of computer tomography. Folia Morphol. 2024; 83(3): 680–688, doi: 10.5603/fm.97820, indexed in Pubmed: 38152919.
32. Roostaeian J, Rohrich RJ, Stuzin JM. Anatomical considerations to prevent facial nerve injury. Plast Reconstr Surg. 2015; 135(5): 1318–1327, doi: 10.1097/PRS.0000000000001244, indexed in Pubmed: 25919245.
33. Sargon MF, Ogretmenoglu O, Gunenc Beser C, et al. Quantitative analysis of the terminal branches of facial nerve in fresh frozen head and neck specimens. Folia Morphol. 2014; 73(1): 24–29, doi: 10.5603/FM.2014.0004, indexed in Pubmed: 24590519.
34. Shokri T, Azizzadeh B, Ducic Y. Modern management of facial nerve disorders. Semin Plast Surg. 2020; 34(4): 277–285, doi: 10.1055/s-0040-1721824, indexed in Pubmed: 33380914.
35. Spencer CR, Irving RM. Causes and management of facial nerve palsy. Br J Hosp Med (Lond). 2016; 77(12): 686–691, doi: 10.12968/hmed.2016.77.12.686, indexed in Pubmed: 27937022.
36. Stankevicius D, Suchomlinov A. Variations in facial nerve branches and anatomical landmarks for its trunk identification: a pilot cadaveric study in the lithuanian population. Cureus. 2019; 11(11): e6100, doi: 10.7759/cureus.6100, indexed in Pubmed: 31886041.
37. Sundaram VK, Schütza V, Schröter NH, et al. Adipo-glial signaling mediates metabolic adaptation in peripheral nerve regeneration. Cell Metab. 2023; 35(12): 2136–2152.e9, doi: 10.1016/j.cmet.2023.10.017, indexed in Pubmed: 37989315.
38. Thuku F, Butt F, Guthua S, et al. An anatomic study of the facial nerve trunk and branching pattern in an african population. Craniomaxillofac Trauma Reconstr Open. 2018; 2(1): s-0038–1669465, doi: 10.1055/s-0038-1669465.
39. Upile T, Jerjes W, Nouraei SA, et al. The stylomastoid artery as an anatomical landmark to the facial nerve during parotid surgery: a clinico-anatomic study. World J Surg Oncol. 2009; 7: 71, doi: 10.1186/1477-7819-7-71, indexed in Pubmed: 19785731.
40. Wegscheider H, Volk GF, Guntinas-Lichius O, et al. High-resolution ultrasonography of the normal extratemporal facial nerve. Eur Arch Otorhinolaryngol. 2018; 275(1): 293–299, doi: 10.1007/s00405-017-4797-z, indexed in Pubmed: 29127505.
41. Witt RL, Weinstein GS, Rejto LK. Tympanomastoid suture and digastric muscle in cadaver and live parotidectomy. Laryngoscope. 2005; 115(4): 574–577, doi: 10.1097/01.mlg.0000161343.85009.4c, indexed in Pubmed: 15805861.
42. Wu X, Li M, Zhang Z, et al. Reliability of preoperative prediction of the location of the facial nerve using diffusion tensor imaging-fiber tracking in vestibular schwannoma: a systematic review and meta-analysis. World Neurosurg. 2021; 146: 351–361.e3, doi: 10.1016/j.wneu.2020.10.136, indexed in Pubmed: 33130136.
43. Zamzam SM, Hassouna M, Elsawy M, et al. Otolaryngologists and iatrogenic facial nerve injury: a meta-analysis. Egypt J Otolaryngol. 2023; 39(1): 71, doi: 10.1186/s43163-023-00440-0.
44. Zhang Y, Mao Z, Wei P, et al. Preoperative prediction of location and shape of facial nerve in patients with large vestibular schwannomas using diffusion tensor imaging-based fiber tracking. World Neurosurg. 2017; 99: 70–78, doi: 10.1016/j.wneu.2016.11.110, indexed in Pubmed: 27915063.
45. Zhong W, Ashwell K. Facial nerve trunk variations with surgical implications: a cadaveric study. Int J Surg Open. 2015; 1: 35–40, doi: 10.1016/j.ijso.2016.02.011.